

## Article

# Depth of Cure, Surface Characteristics, Hardness, and Brushing Wear of 4 Direct Restorative Materials in Paediatric Dentistry

Francesco Saverio Ludovichetti <sup>1,\*</sup>, Angela Guariso <sup>1</sup>, Roberta Gaia Parcianello <sup>2</sup>, Luca Pezzato <sup>3</sup>, Rachele Bertolini <sup>4</sup>, Patrizia Lucchi <sup>1</sup> and Sergio Mazzoleni <sup>1</sup>

<sup>1</sup> Department of Neurosciences—Dentistry Section, University of Padova, 35122 Padova, Italy; angela.guariso@unipd.it (A.G.); patrizia.lucchi@unipd.it (P.L.); sergio.mazzoleni@unipd.it (S.M.)

<sup>2</sup> Department of Biomedical, Surgical and Dental Sciences, University of Milan, 20122 Milano, Italy; roberta.parcianello@unimi.it

<sup>3</sup> Institute of Condensed Matter Chemistry and Energy Technologies (ICMATE), National Research Council of Italy, C.so Stati Uniti 4, 35127 Padova, Italy; luca.pezzato@unipd.it

<sup>4</sup> Department of Industrial Engineering, Università degli Studi di Padova, 35122 Padova, Italy; rachele.bertolini@unipd.it

\* Correspondence: francesco.ludovichetti@unipd.it

**Abstract:** Aim: The study aimed to compare the depth of cure, hardness, surface roughness, and wear resistance of four restorative materials used in pediatric dentistry: FUJI IX GP FAST, RivaSilver, SDR flow+, and Vertise Flow. Materials and Methods: The depth of cure was measured per ISO 4049 standards using a digital caliper, with 15 samples of each material. Hardness was evaluated using a Vickers indenter under a 10 N load for 20 s. Surface roughness was assessed before and after acid exposure using an optical profilometer according to ISO 4288. Brushing wear resistance was analyzed by subjecting samples to 20 and 60 min of brushing, followed by roughness measurements. Statistical analysis was performed using independent sample *t*-tests to determine the significance of differences between the materials, with *p*-values < 0.05 considered significant. Results: SDR flow+ exhibited the highest depth of cure with an average of 3.5 mm ( $\pm 0.2$  mm), significantly higher than Vertise Flow at 2.8 mm ( $\pm 0.3$  mm) ( $p < 0.001$ ). Hardness testing revealed SDR flow+ had the highest average hardness (85 HV  $\pm 4$  HV), while Vertise Flow had the lowest (72 HV  $\pm 5$  HV) ( $p < 0.001$ ). Surface roughness increased significantly after acid exposure for RivaSilver (from 1.2  $\mu\text{m} \pm 0.12 \mu\text{m}$  to 1.6  $\mu\text{m} \pm 0.15 \mu\text{m}$ ,  $p = 0.007$ ) and for SDR flow+ (from 0.85  $\mu\text{m} \pm 0.08 \mu\text{m}$  to 1.3  $\mu\text{m} \pm 0.14 \mu\text{m}$ ,  $p = 0.001$ ). Brushing wear resistance was highest in RivaSilver (Ra increase from 1.2  $\mu\text{m}$  to 1.4  $\mu\text{m} \pm 0.11 \mu\text{m}$ ) and lowest in FUJI IX GP FAST (Ra increase from 1.5  $\mu\text{m}$  to 1.9  $\mu\text{m} \pm 0.15 \mu\text{m}$ ,  $p < 0.001$ ). Conclusions: The study demonstrates significant differences in performance among the tested materials. SDR flow+ showed a superior depth of cure and hardness, making it suitable for high-stress applications. However, all materials displayed increased surface roughness following acid exposure and brushing, with FUJI IX GP FAST showing the highest wear. These findings highlight the need to select restorative materials based on the specific clinical demands of pediatric patients, considering both their mechanical properties and resistance to wear and acid.

**Keywords:** dental materials; pediatric dentistry; depth of cure; hardness; roughness



**Citation:** Ludovichetti, F.S.; Guariso, A.; Parcianello, R.G.; Pezzato, L.; Bertolini, R.; Lucchi, P.; Mazzoleni, S. Depth of Cure, Surface Characteristics, Hardness, and Brushing Wear of 4 Direct Restorative Materials in Paediatric Dentistry. *Appl. Sci.* **2024**, *14*, 8783. <https://doi.org/10.3390/app14198783>

Academic Editor: Hideki Kitaura

Received: 31 August 2024

Revised: 23 September 2024

Accepted: 25 September 2024

Published: 29 September 2024



**Copyright:** © 2024 by the authors. Licensee MDPI, Basel, Switzerland. This article is an open access article distributed under the terms and conditions of the Creative Commons Attribution (CC BY) license (<https://creativecommons.org/licenses/by/4.0/>).

## 1. Introduction

Pediatric dentistry employs a wide range of materials for direct conservative restorations, including glass ionomer cements, composite resins, bulk-fill resins, and self-etching and/or self-adhesive resins. Glass ionomer cements are materials formed from a reaction between a powder and liquid, which prove highly useful in pediatric dentistry due to their ease of manipulation and fluoride release capabilities [1]. They offer a protective effect on the tooth surface, are bioactive, and are suited to various applications, including dental restorations. In addition to their fluoride-releasing ability, these materials also adhere

well to tooth structures, but some studies suggest their main disadvantages include wear and long-term strength loss [2]. Currently, composite resins are the most widely used material for treating carious lesions on permanent teeth, gradually replacing the use of dental amalgam due to their biocompatibility, good aesthetic quality, easier handling, and non-toxicity [3]. Composite resins consist of three primary components: a polymeric resin matrix, a filler, and a coupling agent that binds the filler to the matrix. Their major drawbacks include polymerization shrinkage, low wear resistance (especially in first-generation composite resins), and a lack of antibacterial activity [4]. The introduction of new materials has led to numerous advantages. For instance, bulk-fill resins can be placed in increments of 4 mm, larger than the 2 mm required for traditional resins, thus avoiding the layering technique while still achieving adequate polymerization [5]. More recently, self-adhesive and self-etching resins have been developed, potentially offering a time-saving advantage in cases of reduced patient cooperation. These composites are used in small Class I cavities, either as a base layer or a sealant without the need for a bonding agent [6]. Currently, three self-adhesive flowable composites are available, including Kerr Vertise Flow, which contains glycerol phosphate dimethacrylate (GPDM) monomers, ensuring a strong etching effect [7]. When selecting an appropriate material, various factors must be considered, including the material's mechanical and physical characteristics. Important considerations include polymerization depth, surface hardness, and roughness, as well as the material's response to acidic attacks and wear [8]. Polymerization depth can be defined as the thickness of resin that can be converted from monomer to polymer and depends on multiple factors, such as the type of material, the amount of filler present, exposure, irradiation, and the distance of the light source in photopolymerizable materials [9]. Inadequate polymerization can lead to restoration failure and subsequent pulpal damage. Hardness refers to the material's resistance to mechanical indentation by a harder object [10]. It is also important to consider roughness, which, in addition to being intrinsic to the material, can increase due to brushing, and increased roughness correlates with increased plaque deposition [11]. In pediatric patients, frequent consumption of acidic foods can cause, in addition to damage to dental tissue, a loss of material strength in restorations. Furthermore, the wear resistance that develops from continual brushing on the dental material is crucial to avoid fractures or restoration loss [12,13]. The purpose of this study is to analyze and compare the polymerization depth, hardness, roughness, and surface characteristics following acidic attack and brushing-induced wear of four materials used in direct restorations in pediatric dentistry. Specifically, the characteristics of two glass ionomer materials, one bulk-fill resin, and one self-etching and self-adhesive resin will be examined.

## 2. Materials and Methods

In this *in vitro* study, the following four materials used for direct restorations in pediatric dentistry were analyzed:

**RivaSilver:** SDI Limited, 5-9 Brunsdon Street, Bayswater, Victoria 3153, Australia.

**SDR flow+:** Dentsply Sirona, 13320 Ballantyne Corporate Place, Charlotte, NC 28277, USA.

**Vertise Flow:** Kerr, 1717 West Collins Avenue, Orange, CA 92867, USA.

**FUJI IX GP FAST:** GC EUROPE N.V., Interleuvenlaan 33, 3001 Leuven, Belgium.

FUJI IX GP FAST is a glass ionomer, while Riva Silver is a silver-reinforced glass ionomer. SDR flow+ is a bulk-fill resin cement, and Vertise Flow is a self-etching, self-adhesive composite resin. For the experimental setup, 15 samples of each material were created using a stainless steel mold with a cavity measuring 4 mm in diameter and 10 mm in length (Figure 1). The mold was filled with the material, ensuring uniform distribution and minimal air bubble incorporation. The top and bottom surfaces were leveled and smoothed using 0.05 mm Mylar sheets. For SDR flow+ and Vertise Flow, a wireless Cheese 5 w photopolymerization lamp (Guilin Woodpecker Medical Instrument Co., Guilin, China) was used to apply light curing for 20 s on each side, whereas FUJI IX and Riva Silver were allowed to set without light exposure. Once set, the cylindrical samples were carefully

removed using a specialized tool (Beta) made of the same material as the mold and matching the diameter of the samples to avoid damaging them.



**Figure 1.** Stainless steel mold containing an opening hole with a diameter of 4 mm and a length of 10 mm, and a Beta tool for removing samples from the cylinder.

### 2.1. Polymerization Depth

The polymerization depth for SDR flow+ and Vertise Flow was investigated using the ISO 4049 method [14–18]. Fifteen samples per material were measured using a digital caliper (Figure 2) with a precision of  $\pm 0.1$  mm. Three measurements were taken per sample, resulting in a total of forty-five measurements per material. The absolute lengths obtained for each material were then halved to calculate the depth of cure (DOC).



**Figure 2.** Digital caliper.

### 2.2. Hardness

Microhardness testing was conducted using a Vickers diamond indenter under a load of 10 N and a dwell time of 20 s [15]. Hardness values (in GPa) were calculated using the formula  $H = p/2d^2$ , where “ $p$ ” is the applied load and “ $d$ ” is the average of the diagonal measurements [19].

### 2.3. Wear Resistance

Wear resistance of the materials was evaluated using four samples per material. Two samples from each material were brushed using an electric toothbrush with soft bristles set at a 40-degree angle and rotating at 6000 rpm for 20 min. Another set of two samples per material was brushed for 60 min to compare the effects. A brushing force of 2 N was applied.

### 2.4. Acid Resistance

To simulate the demineralization process, a carbonated beverage (Coca Cola<sup>®</sup>, Atlanta, GA, USA) was used. The pH, buffering capacity, and concentrations of calcium and

phosphate were measured at 20 °C and averaged over three tests. Two samples per material were immersed in 5 mL of the beverage for 2 min at room temperature and then rinsed with deionized water. This immersion procedure was repeated four times for a total exposure of 8 min. Additional tests involved applying fluoride toothpaste over the entire surface of two other samples, followed by another acid immersion [16–20]. After that, surface roughness was measured as follows.

### 2.5. Surface Roughness

Surface roughness (Ra) was measured using a Sensofar Plu Neox optical profilometer (Barcelona, Spain). Lateral scans of  $1.3 \times 0.6 \text{ mm}^2$  were acquired using a  $20\times$  confocal objective. Three scans were performed on different areas of each sample, and three surface profiles were extracted from each scan. Roughness was calculated according to ISO 4288 [21] using two filters, namely  $\lambda$  and  $\lambda_c$ , set at  $2.5 \mu\text{m}$  and  $0.025 \text{ mm}$ , respectively.

### 2.6. Scanning Electron Microscopy (SEM)

The surfaces of samples analyzed for surface roughness and wear resistance were examined using a Cambridge Stereoscan 440 SEM (Leica Microsystems, Milan, Italy) coated with a 20 nm gold layer to enhance conductivity. A Philips PV9800 EDS microanalysis system was also used for detailed examination. Images were captured using a secondary electron detector [17].

### 2.7. Statistical Analysis

For each analyzed parameter, an independent sample *t*-test was used to compare the means of two separate groups. Specifically, the variable ‘Value’ was compared across different groups categorized by the variable ‘Type’. The *t*-test was applied to determine if there is a statistically significant difference between the group means. A *p*-value less than 0.001 indicates that the observed difference between the means is highly unlikely to occur by chance, suggesting strong statistical significance.

## 3. Results

### 3.1. Polymerization Depth

The depth of cure (DOC) was assessed for both SDR flow+ and Vertise Flow, and the measurements are presented in Table 1. SDR flow+ demonstrated a greater average DOC of 3.5 mm ( $\pm 0.2 \text{ mm}$ ) compared to Vertise Flow, which showed an average DOC of 2.8 mm ( $\pm 0.3 \text{ mm}$ ). This difference was found to be statistically significant with a *p*-value of  $<0.001$ , as illustrated in Figure 3. These results clearly indicate that SDR flow+ allows for a deeper polymerization within a single increment. The higher DOC observed for SDR flow+ is consistent across all samples, suggesting that this material may be particularly effective for applications requiring deeper curing.

**Table 1.** Three measurements for each material, obtained using a digital caliper, and the average of the measurements for calculating the polymerization depth.

Vertise Flow	Meas.1	Meas.2	Meas.3	Mean	SDR Flow+	Meas.1	Meas.2	Meas.3	Mean
1	2.49	2.45	2.38	2.44	1	3.86	4.02	3.99	3.96
2	2.35	2.51	2.35	2.40	2	4.23	4.41	4.3	4.31
3	2.3	2.37	2.49	2.38	3	3.53	3.56	3.61	3.56
4	2.12	2.2	2.10	2.14	4	4.15	4.12	4.11	4.12
5	2.28	2.37	2.43	2.36	5	3.80	3.79	3.74	3.78
6	2.27	2.46	2.44	2.39	6	3.99	3.86	4.01	3.94
7	2.65	2.56	2.22	2.48	7	4.18	4.11	3.98	4.10
8	2.58	2.64	2.6	2.60	8	3.96	4.08	4.11	4.05
9	2.65	2.58	2.62	2.61	9	4.47	4.49	4.30	4.42
10	2.77	2.76	2.68	2.74	10	4.27	4.37	4.25	4.3

Table 1. Cont.

Vertise Flow	Meas.1	Meas.2	Meas.3	Mean	SDR Flow+	Meas.1	Meas.2	Meas.3	Mean
11	2.47	2.64	2.37	2.49	11	3.88	3.86	3.85	3.85
12	3.05	3.06	2.97	3.04	12	4.51	4.39	4.4	4.43
13	2.29	2.25	2.29	2.27	13	3.71	3.66	3.95	3.77
14	1.94	2.05	2.06	2.01	14	3.95	3.93	3.75	3.88
15	2.27	2.17	2.24	2.22	15	4.09	4.13	4.1	4.10

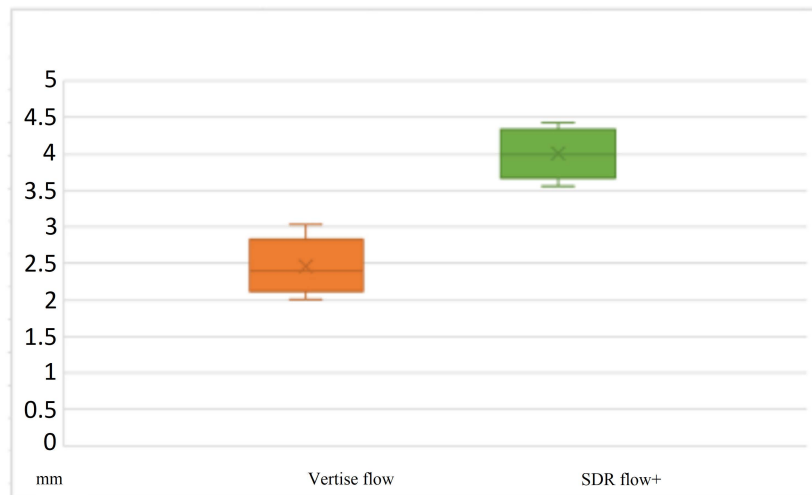


Figure 3. Boxplot SDR flow+ and Vertise Flow.

### 3.2. Hardness

Microhardness testing was conducted on all four materials, with the results summarized in Tables 2 and 3. FUJI IX GP FAST showed an average hardness value of 80 HV ( $\pm 5$  HV), while RivaSilver exhibited a similar average hardness of 78 HV ( $\pm 6$  HV). The difference between these two glass ionomer materials was not statistically significant ( $p = 0.125$ ), indicating comparable hardness characteristics. Conversely, SDR flow+ showed a significantly higher average hardness value of 85 HV ( $\pm 4$  HV), compared to 72 HV ( $\pm 5$  HV) for Vertise Flow, with a  $p$ -value of  $<0.001$ . These hardness values are presented in detail in the corresponding box plots, demonstrating the variability and consistency of each material’s performance. The data suggest that SDR flow+ has a higher resistance to indentation compared to the other materials tested.

Table 2. Hardness values for the four materials, measured in Vickers units (HV).

	No Treatment (A) (Mean and Dv. Std.)	20 min Brushing (B) (Mean and Dv. Std.)	60 min Brushing (C) (Mean and Dv. Std.)
RivaSilver	90 $\pm$ 3	110 $\pm$ 4	110 $\pm$ 5
SDR Flow+	515 $\pm$ 10	401 $\pm$ 12	480 $\pm$ 15
Vertise Flow	498 $\pm$ 8	439 $\pm$ 7	426 $\pm$ 9
FUJI IX GP FAST	92 $\pm$ 2	110 $\pm$ 3	116 $\pm$ 14

Table 3.  $p$ -value in the hardness comparison of various materials for different groups.

Experiment Number	Group 1	Group 2	$p$ -Value
1	FUJI IX GP FAST	RivaSilver	$<0.001$
1	FUJI IX GP FAST	SDR flow+	$<0.001$
1	RivaSilver	SDR flow+	$<0.001$
1	FUJI IX GP FAST	Vertise Flow	$<0.001$

Table 3. Cont.

Experiment Number	Group 1	Group 2	p-Value
1	RivaSilver	Vertise Flow	<0.001
1	SDR flow+	Vertise Flow	<0.001
2	FUJI IX GP FAST	RivaSilver	0.125
2	FUJI IX GP FAST	SDR flow+	<0.001
2	RivaSilver	SDR flow+	<0.001
2	FUJI IX GP FAST	Vertise Flow	<0.001
2	RivaSilver	Vertise Flow	<0.001
2	SDR flow+	Vertise Flow	<0.001
3	FUJI IX GP FAST	RivaSilver	<0.001
3	FUJI IX GP FAST	SDR flow+	<0.001
3	RivaSilver	SDR flow+	<0.001
3	FUJI IX GP FAST	Vertise Flow	<0.001
3	RivaSilver	Vertise Flow	<0.001
3	SDR flow+	Vertise Flow	<0.001

### 3.3. Surface Roughness after Acid Treatment

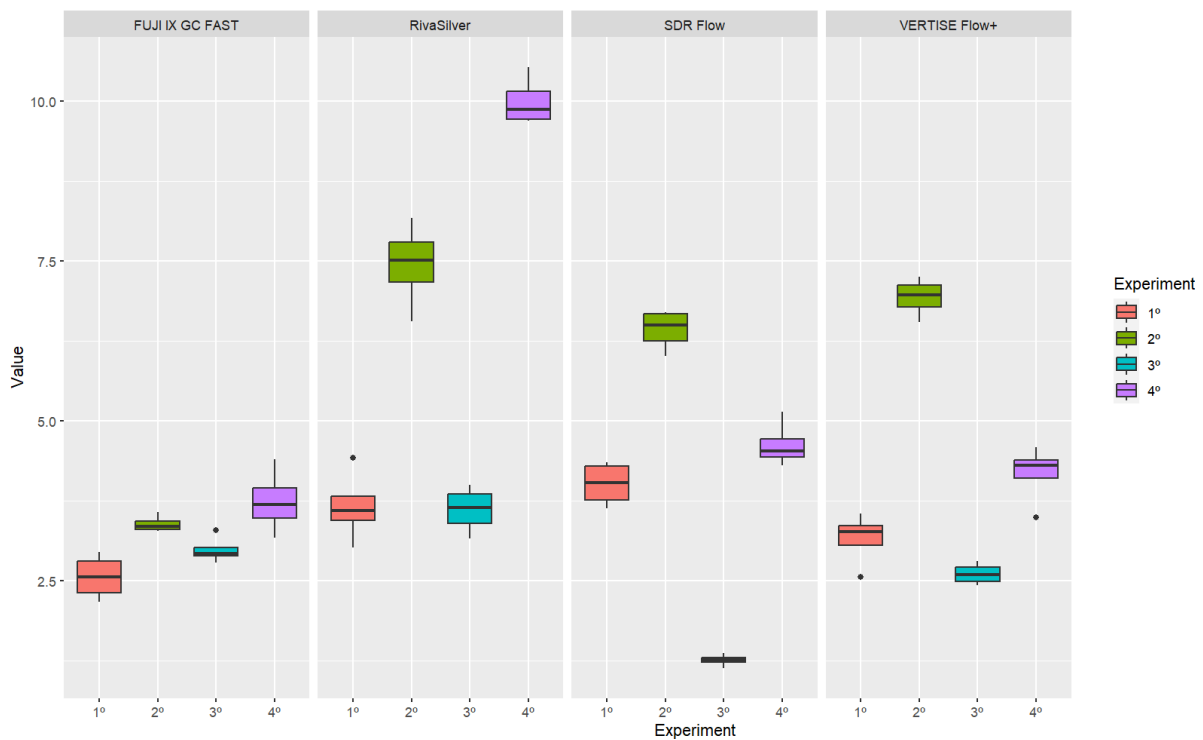
Surface roughness (Ra) measurements were taken before and after acid treatment to simulate the effects of acidic exposure on the materials. The results are detailed in Tables 4 and 5 and illustrated in Figure 4. FUJI IX GP FAST exhibited minimal change in surface roughness after acid treatment, with values of 0.95  $\mu\text{m}$  ( $\pm 0.10 \mu\text{m}$ ) before treatment and 0.97  $\mu\text{m}$  ( $\pm 0.09 \mu\text{m}$ ) after, showing no statistically significant difference ( $p = 0.133$ ). On the other hand, RivaSilver showed a significant increase in roughness from 1.2  $\mu\text{m}$  ( $\pm 0.12 \mu\text{m}$ ) to 1.6  $\mu\text{m}$  ( $\pm 0.15 \mu\text{m}$ ) post-acid exposure ( $p = 0.007$ ). SDR flow+ and Vertise Flow also demonstrated significant increases in surface roughness following acid treatment, with SDR flow+ roughness increasing from 0.85  $\mu\text{m}$  ( $\pm 0.08 \mu\text{m}$ ) to 1.3  $\mu\text{m}$  ( $\pm 0.14 \mu\text{m}$ ) ( $p = 0.001$ ) and Vertise Flow increasing from 0.88  $\mu\text{m}$  ( $\pm 0.09 \mu\text{m}$ ) to 1.4  $\mu\text{m}$  ( $\pm 0.13 \mu\text{m}$ ) ( $p = 0.005$ ). The SEM images in Figure 5 provide visual evidence of the surface alterations observed post-treatment.

Table 4. Roughness values, highlighting statistically significant comparisons between materials after acid treatment.

Variabile	Group 1	Group 2	p-Value
FUJI IX GP FAST	1	2	0.068
FUJI IX GP FAST	1	3	0.246
FUJI IX GP FAST	1	4	0.340
FUJI IX GP FAST	2	3	0.251
FUJI IX GP FAST	2	4	1.000
FUJI IX GP FAST	3	4	0.588
RivaSilver	1	2	0.007
RivaSilver	1	3	1.000
RivaSilver	1	4	0.003
RivaSilver	2	3	0.022
RivaSilver	2	4	0.050
RivaSilver	3	4	0.002
SDR flow+	1	2	0.000
SDR flow+	1	3	0.002
SDR flow+	1	4	1.000
SDR flow+	2	3	0.000
SDR flow+	2	4	0.076
SDR flow+	3	4	0.003
Vertise Flow	1	2	0.005
Vertise Flow	1	3	0.281
Vertise Flow	1	4	0.001
Vertise Flow	2	3	0.002
Vertise Flow	2	4	0.016
Vertise Flow	3	4	0.027

**Table 5.** Roughness values for the four groups analyzed after acid treatment, highlighting statistically significant differences.

Experiment Number	Group 1	Group 2	p-Value
1	FUJI IX GP FAST	RivaSilver	0.019
1	FUJI IX GP FAST	SDR flow+	0.003
1	RivaSilver	SDR flow+	0.276
1	FUJI IX GP FAST	Vertise Flow	0.226
1	RivaSilver	Vertise Flow	0.261
1	SDR flow+	Vertise Flow	0.069
2	FUJI IX GP FAST	RivaSilver	0.001
2	FUJI IX GP FAST	SDR flow+	0.001
2	RivaSilver	SDR flow+	0.013
2	FUJI IX GP FAST	Vertise Flow	0.001
2	RivaSilver	Vertise Flow	0.211
2	SDR flow+	Vertise Flow	0.211
3	FUJI IX GP FAST	RivaSilver	0.005
3	FUJI IX GP FAST	SDR flow+	0.001
3	RivaSilver	SDR flow+	0.001
3	FUJI IX GP FAST	Vertise Flow	0.043
3	RivaSilver	Vertise Flow	0.000
3	SDR flow+	Vertise Flow	0.001
4	FUJI IX GP FAST	RivaSilver	0.001
4	FUJI IX GP FAST	SDR flow+	0.042
4	RivaSilver	SDR flow+	0.001
4	FUJI IX GP FAST	Vertise Flow	0.339
4	RivaSilver	Vertise Flow	0.001
4	SDR flow+	Vertise Flow	0.339



**Figure 4.** Boxplot of surface roughness of the four acid groups.



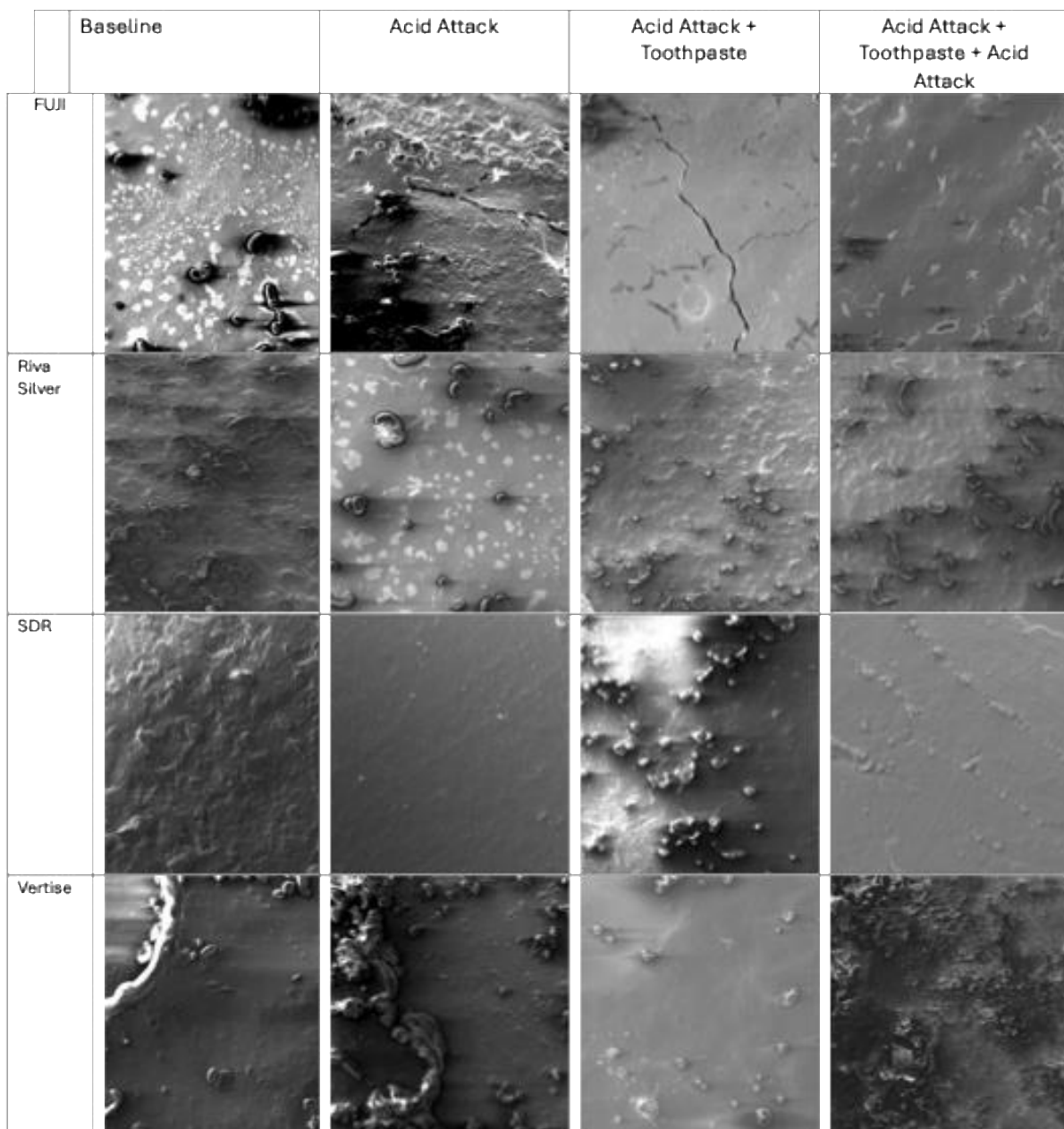


**Figure 5.** SEM of the 4 materials subjected to different acid treatments, magnification 500 $\times$ .

### 3.4. Brushing Wear Resistance

Brushing wear resistance was assessed by measuring surface roughness before and after 20 and 60 min of brushing. The detailed results are found in Tables 6–8, with visual representations provided in Figures 6 and 7. RivaSilver exhibited the lowest increase in roughness after 60 min of brushing, with Ra values rising from 1.2  $\mu\text{m}$  to 1.4  $\mu\text{m}$  ( $\pm 0.11 \mu\text{m}$ ). In contrast, FUJI IX GP FAST showed the most significant increase in roughness, with values increasing from 1.5  $\mu\text{m}$  to 1.9  $\mu\text{m}$  ( $\pm 0.15 \mu\text{m}$ ) ( $p < 0.001$ ). SDR flow+ and Vertise Flow also experienced increases in surface roughness after brushing; SDR flow+ roughness increased from 1.0  $\mu\text{m}$  ( $\pm 0.09 \mu\text{m}$ ) to 1.5  $\mu\text{m}$  ( $\pm 0.12 \mu\text{m}$ ) ( $p = 0.008$ ), while Vertise Flow's roughness increased from 1.1  $\mu\text{m}$  ( $\pm 0.10 \mu\text{m}$ ) to 1.6  $\mu\text{m}$  ( $\pm 0.13 \mu\text{m}$ ) ( $p = 0.001$ ). These findings are comprehensively detailed in Tables 7 and 8, which capture the variability and extent of wear among the different materials.



**Table 6.** Roughness values of the four materials subjected to different types of brushing treatment.

Specimen	Riughness Values				Mean	Standard Deviation
	Ra 1	Ra 2	Ra 3	Ra 4		
RivaSilver I	4.42	3.58	3.021	3.619	3.660	0.576
SDR Flow I	6.014	6.701	6.668	6.329	6.428	0.323
VERTISE Flow+ I	6.546	7.074	6.861	7.254	6.934	0.304
FUJI IX GP FAST I	2.756	2.948	2.356	2.167	2.557	0.358
Rivasilver II	8.164	7.667	7.363	6.558	7.438	0.673
SDR Flow+ II	3.63	4.352	4.272	3.796	4.013	0.354
Vertise Flow II	3.553	3.301	2.561	3.218	3.158	0.423
FUJI IX GP FAST II	3.574	3.38	3.276	3.307	3.384	0.134
Rivasilver III	9.695	10.53	9.721	10.023	9.992	0.388
SDR Flow+ III	5.137	4.48	4.306	4.578	4.625	0.359
Vertise Flow III	4.591	4.3	3.486	4.316	4.173	0.477
FUJI IX GP FAST III	3.174	3.574	4.391	3.798	3.734	0.508
RivaSilver IV	3.477	3.154	3.991	3.807	3.607	0.369
SDR Flow+ IV	1.253	1.263	1.369	1.132	1.254	0.097
Vertise Flow IV	2.801	2.681	2.503	2.423	2.602	0.171
FUJI IX GP FAST IV	2.921	3.291	2.786	2.917	2.979	0.217

**Table 7.** *p*-values in the comparison of various materials for different brushing treatments.

Experiment Number	Group 1	Group 2	<i>p</i> -Value
1	FUJI IX GP FAST	RivaSilver	<0.001
1	FUJI IX GP FAST	SDR flow+	<0.001
1	RivaSilver	SDR flow+	0.442
1	FUJI IX GP FAST	Vertise Flow	0.0032
1	RivaSilver	Vertise Flow	<0.001
1	SDR flow+	Vertise Flow	<0.001
2	FUJI IX GP FAST	RivaSilver	<0.001
2	FUJI IX GP FAST	SDR flow+	<0.001
2	RivaSilver	SDR flow+	<0.001
2	FUJI IX GP FAST	Vertise Flow	<0.001
2	RivaSilver	Vertise Flow	<0.001
2	SDR flow+	Vertise Flow	0.754

**Table 8.** Roughness values for brushing at 20 or 60 min.

	Roughness (μm)				Mean (μm)	Standard Dev. (μm)
	Ra 1	Ra 2	Ra 3	Ra 4		
Riva silver 1	3.27	3.14	3.49	3.12	3.26	0.17
SDR flow 1	3.20	3.35	3.50	3.47	3.38	0.14
Vertise Flow 1	4.25	4.98	5.09	4.89	4.80	0.38
FUJI IX GP FAST 1	5.54	5.49	5.37	5.36	5.44	0.09
Riva silver 2	3.24	3.39	3.14	3.32	3.27	0.11
SDR Flow+ 2	6.02	5.97	6.13	5.96	6.02	0.08
Vertise Flow 2	6.07	6.05	6.18	5.87	6.04	0.13
FUJI IX GP FAST 2	5.43	5.33	5.40	5.27	5.36	0.07

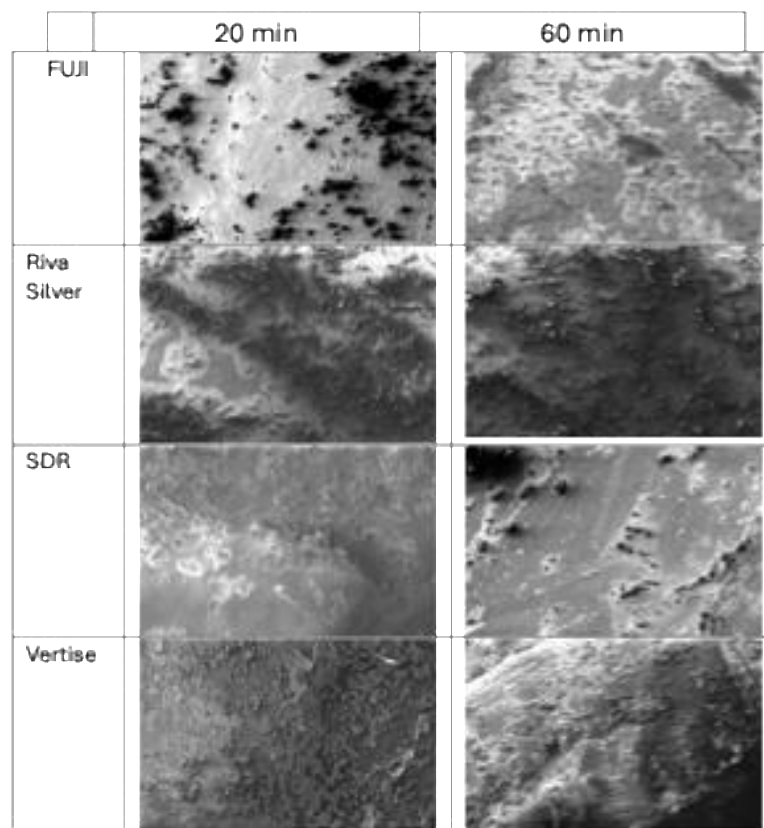


Figure 6. SEM of the 4 materials subjected to different brushing times, magnification 500×.

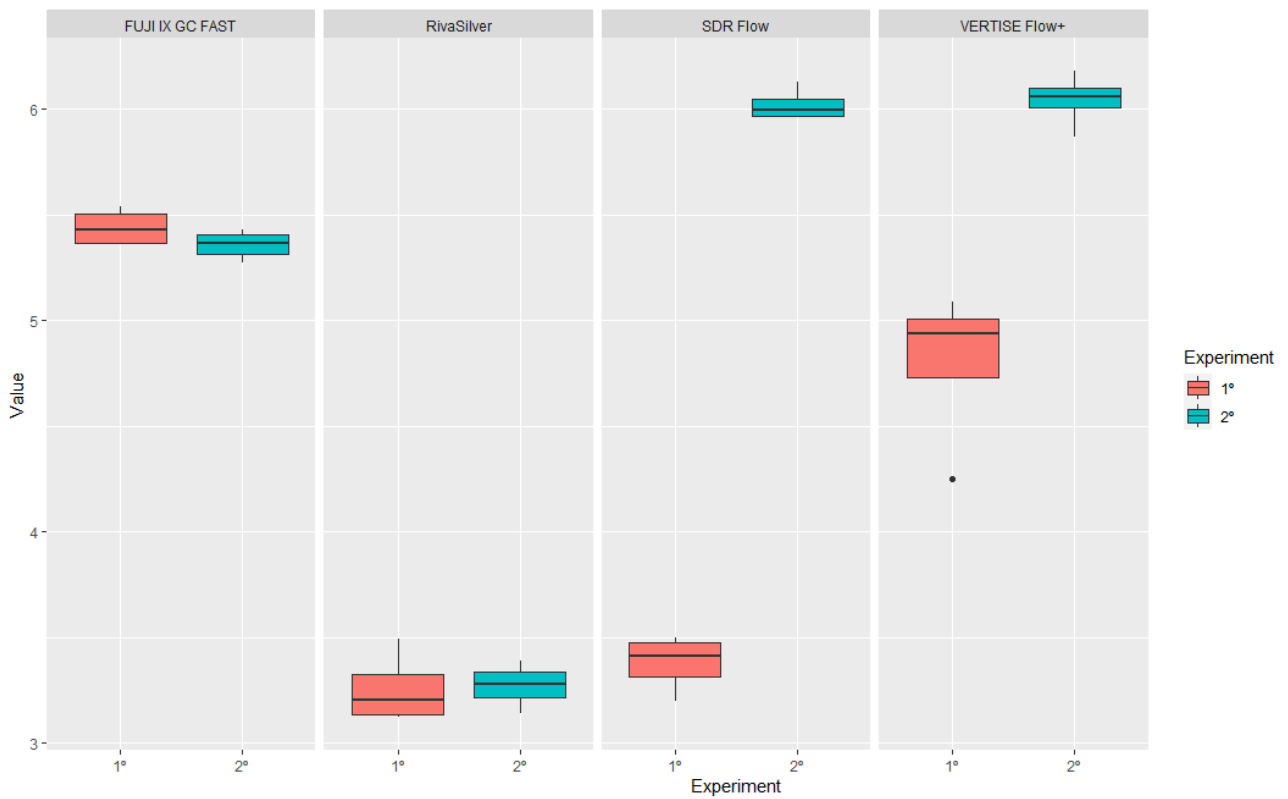


Figure 7. Boxplot of roughness due to brushing of the two groups.

#### 4. Discussion

This study aimed to compare various materials used in pediatric dentistry by evaluating key properties, such as polymerization depth, hardness, roughness, and surface characteristics after acid exposure and wear. The results show that SDR flow+ exhibits a significant depth of cure (DOC), resulting in low polymerization shrinkage. These findings align with the characteristics typically associated with bulk-fill resins, as supported by the study conducted by Ludovichetti et al. (2022) [22].

In this investigation, the DOC of several highly filled flowable composites and bulk-fill composites was assessed. Samples with a diameter and depth of 4 mm were polymerized for 20 s and subsequently stored in water for 24 h. The bulk-fill composites consistently demonstrated low polymerization shrinkage stress alongside a favorable DOC. Notably, the comparison between SDR flow+ and Vertise Flow revealed a superior DOC in the bulk-fill resin, a result corroborated by Sampaio et al. (2017) [23]. In their referenced study, standardized Class I preparations (2.5 mm depth × 4 mm length × 4 mm width) were performed on 24 caries-free human third molars using a traditional composite, two bulk-fill composites, and a self-adhesive resin. Each tooth was scanned thrice with a microcomputed tomography instrument, and the percentage of volumetric polymerization shrinkage was calculated. The bulk-fill resin composite exhibited the lowest volumetric shrinkage values. The enhancement of DOC in bulk-fill resins is attributed to modifications in filler content and the organic matrix, with the size and amount of filler influencing light transmission [24,25]. Furthermore, the existing literature consistently reports a lower DOC in self-adhesive resins compared to bulk-fill resins.

The microhardness test results indicate that the hardness values of the two glass ionomer cements remained nearly unchanged after brushing, contrary to the other two materials, which exhibited a reduction in hardness, particularly after extended brushing. Specifically, Vertise Flow demonstrated a lower hardness value than the other materials, with a more pronounced decrease after brushing. A lower surface microhardness is linked to decreased wear resistance and the potential for material damage, which can compromise fatigue resistance and lead to restoration failure [26]. The observation of low hardness in self-adhesive resin aligns with the findings of Azizi et al. (2023) [27]. In their *in vitro* study, 50 samples with dimensions of 10 mm × 10 mm × 2 mm were prepared, including 3 conventional flowable composites, one microhybrid composite, and Vertise Flow, a self-adhesive flowable composite. After polishing, the microhardness was measured using a Vickers hardness tester, and the samples were subjected to various wear cycles [28]. The analysis confirmed that Vertise Flow had the lowest hardness value.

However, a study by Czasch et al. (2013) reported good hardness values for Vertise Flow when compared with two other composite resins. The samples were of various sizes, and hardness was analyzed using the Vickers test. The material's hardness is attributed to its inorganic components, including barium glass, colloidal silica, and ytterbium fluoride, which constitute approximately 70% of the total weight—a higher percentage than in other resins examined in the study [29]. The high microhardness values of RivaSilver are consistent with the findings of Cabello Malagón et al. (2022) [30], who reported that RivaSilver exhibited the highest microhardness value among glass ionomer cements, likely due to the addition of silver particles. According to Yin et al. (2020), these particles enhance the mechanical properties of the cement and provide an antibacterial effect [31,32]. Cabello Malagón et al. (2022) analyzed 4 mm × 6 mm samples, which were sectioned and tested for hardness using a Vickers indenter, applying a 100 g load for 15 s. This study demonstrates that FUJI IX GP FAST and RivaSilver achieved comparable hardness values, with FUJI IX GP FAST showing slightly higher values. Both were superior to bulk-fill and self-adhesive resins, highlighting the durability of glass ionomer cements in pediatric dentistry, even after wear from brushing. This supports their application in pediatric dentistry. The response of materials to acid exposure revealed that toothpaste offered some protective effects, but only in specific instances. The roughness was analyzed using an optical profilometer, the standard method for assessing tissue loss *in vitro* and *in situ* during

erosion simulations [33]. The application of toothpaste after the first demineralization cycle on RivaSilver and FUJI IX GP FAST did not decrease roughness but instead increased it. However, after two demineralization cycles, a protective effect was observed. These findings contrast with the study by Mulic et al. (2016) [34], which evaluated the effectiveness of various toothpastes on glass ionomer cement restorations made on extracted bovine teeth, subjected to demineralization cycles, and assessed for wear at the enamel–cement interface. In that study, no positive effect of toothpaste was noted after multiple demineralization processes. However, the materials and experimental conditions differed from those in the present study, with the acid process simulated over five days and samples immersed in 250 mL of citric acid, shaken on an orbital shaker while a toothpaste and distilled water mixture was applied for two minutes at hourly intervals. The samples were also immersed in artificial saliva throughout the experiment [14,35].

FUJI IX GP FAST exhibited low roughness values, a result that contradicts the findings of Cruz et al. (2015) [36], where the analyzed glass ionomer had the highest roughness values compared to other materials. However, the glass ionomer was compared with different materials, including giomer, amalgomer, and glass carbomer, which differ significantly from those examined in this study. Conversely, SDR flow+ resin, consistent with Kelten et al. (2020), displayed high roughness values, which may be due to its lower filler content and the polymerization modulator chemically incorporated into the center of the polymerizable resin [37]. This study analyzed various bulk-fill composites by creating 30 disc-shaped samples (10 mm × 12 mm) using a stainless steel mold and Mylar sheets to ensure material uniformity. The samples were photopolymerized for 20 s, followed by surface roughening and polishing, with the roughness measured using a profilometer [38]. Overall, resin-containing materials, such as SDR flow+ and Vertise Flow, showed lower surface roughness values after acid attacks compared to RivaSilver, a resin-free glass ionomer cement. This finding aligns with Marghalani (2010), who stated that filler particles enhance the mechanical strength of materials, a crucial factor for posterior restorations [39]. This study underscores the need for further research on RivaSilver and FUJI IX GP FAST, given that their roughness values deviated from the typical behavior of other glass ionomer cements. There is limited scientific literature on these materials, particularly in comparison to other non-glass ionomer materials.

Furthermore, roughness due to wear revealed different values compared to those recorded after acid exposure. Notably, after both 20 and 60 min of brushing, RivaSilver recorded the lowest roughness values, followed by SDR flow+ and Vertise Flow, while FUJI IX GP FAST recorded the highest values overall. These results diverge from those of Yap et al. (2000), who, in comparing the wear resistance of glass ionomer restorative materials, concluded that the wear resistance of FUJI IX GP FAST was comparable to that of metal-reinforced GIC, microfilled, and minifilled composites [40]. The low roughness of RivaSilver after brushing is consistent with the findings of Dionysopoulos et al. (2017), who analyzed the response of two glass ionomers to brushing with a commercial toothbrush at a frequency of 1.25 Hz for 10,000 cycles, reporting a reduction in surface roughness following the treatment [41].

In contrast, SDR flow+ and Vertise Flow both recorded increased roughness values after 20 and 60 min of brushing. The roughness data for Vertise Flow is consistent with Ruivo et al. (2019), where Vertise Flow exhibited high roughness values after samples were brushed with aluminum oxide discs and analyzed with a profilometer. Compared to other materials, including a nanofilled composite resin and other flowable composite materials, Vertise Flow likely displayed higher roughness due to its lower filler load and greater water absorption and solubility [42,43]. The roughness observed for SDR flow+ aligns with O'Neill et al. (2018), where samples were prepared in a mold with a diameter of 12.7 mm and a depth of 2 mm, then subjected to brushing by a customized brushing unit (Ultradent) with a consistent predetermined load while rotating the samples. An increase in SDR flow+ roughness was recorded after brushing [44].

## 5. Limitation of the Study

A limitation of this study is the use of paired *t*-tests for multiple comparisons, which may increase the risk of Type I errors, leading to potential false-positive results. Although paired *t*-tests were employed to compare related groups, the risk of inflated Type I errors must be acknowledged. Future studies could benefit from using more robust statistical methods, such as ANOVA with post hoc testing, to control for multiple comparisons in a systematic way. Additionally, applying corrections, like the Bonferroni correction, could also help mitigate this issue. However, these adjustments can reduce statistical power and increase the risk of Type II errors, which should also be considered.

## 6. Conclusions

This study highlights significant differences in the performance of various dental materials used in pediatric dentistry, particularly under conditions of wear and acid exposure. Bulk-fill materials, like SDR flow+ demonstrated superior depth of cure and maintained structural integrity under stress, making them suitable for restorations in high-stress areas. On the other hand, glass ionomer cements, despite their good hardness, showed higher susceptibility to surface degradation in acidic environments, suggesting they may be less ideal in such conditions. Clinically, these findings suggest that bulk-fill materials could be preferable for pediatric restorations requiring durability against mechanical and chemical stress. However, glass ionomer cements might still be appropriate where fluoride release and aesthetics are prioritized, with careful consideration of their potential vulnerability to acid. Further *in vivo* studies are needed to validate these results and refine material selection in pediatric dentistry.

**Author Contributions:** Conceptualization, F.S.L. and S.M.; methodology, L.P. and R.B.; software, R.B.; validation, F.S.L., P.L. and S.M.; formal analysis, L.P. and R.B.; investigation, A.G.; resources, F.S.L. and S.M.; data curation, R.B.; writing—original draft preparation, R.G.P.; writing—review and editing, F.S.L.; visualization, P.L.; supervision, S.M. All authors have read and agreed to the published version of the manuscript.

**Funding:** This research received no external funding.

**Institutional Review Board Statement:** Not applicable.

**Informed Consent Statement:** Not applicable.

**Data Availability Statement:** The original contributions presented in the study are included in the article, further inquiries can be directed to the corresponding author.

**Conflicts of Interest:** The authors declare no conflicts of interest.

## References

1. Donly, K.J. Restorative dentistry for children. *Dent. Clin. N. Am.* **2013**, *57*, 75–82. [[CrossRef](#)] [[PubMed](#)]
2. Nowak, A.; Christensen, J.; Mabry, T.; Townsend, J.; Wells, M. *Pediatric Dentistry: Infancy through Adolescence*, 6th ed.; Elsevier: Philadelphia, PA, USA, 2019; p. 295.
3. Tortora, G.; Farronato, M.; Gaffuri, F.; Carloni, P.; Occhipinti, C.; Tucci, M.; Cenzato, N.; Maspero, C. Survey of oral hygiene habits and knowledge among school children: A cross-sectional study from Italy. *Eur. J. Paediatr. Dent.* **2023**, *24*, 194–200. [[PubMed](#)]
4. Almuhaiza, M. Glass-ionomer cements in restorative dentistry: A critical appraisal. *J. Contemp. Dent. Pract.* **2016**, *17*, 331–336. [[CrossRef](#)] [[PubMed](#)]
5. Rachmia Riva, Y.; Fauziyah Rahman, S. Dental composite resin: A review. *AIP Conf. Proc.* **2019**, *2193*, 020011.
6. Gupta, R.; Hegde, J.; Prakash, V.; Sreirekha, A. *Concise Conservative Dentistry and Endodontics*; Elsevier: Chennai, India, 2019; pp. 260–268.
7. Shen, C.; Rawls, H.R.; Esquivel-Upshaw, J.F. *Phillippe's Science of Dental Materials*; Elsevier: Amsterdam, The Netherlands, 2022; pp. 89–104.
8. Li, X.; Pongprueksa, P.; Meerbeek, B.V.; De Munck, J. Curing profile of bulk-fill resin-based composites. *J. Dent.* **2015**, *43*, 664–672. [[CrossRef](#)]
9. Celik, E.U.; Kucukyilmaz, E.; Savas, S. Effect of different surface pre-treatment methods on the microleakage of two different self-adhesive composites in Class V cavities. *Eur. J. Paediatr. Dent.* **2015**, *16*, 33–38.
10. Ilie, N.; Hickel, R. Resin composite restorative materials. *Aust. Dent. J.* **2011**, *56*, 59–66. [[CrossRef](#)]

11. Schneider, L.; Cavalcante, L.; Silikas, N. Shrinkage stresses generated during resin-composite applications: A review. *J. Dent. Biomech.* **2020**, *2020*, 131630. [[CrossRef](#)]
12. Riggio, M.; Piazza, M.; Kasal, B.; Tannert, T. Hardness test in situ assessment of structural timber. In *RILEM State of the Art Reports*; Springer: Dordrecht, The Netherlands, 2012; Volume 7.
13. Heintze, S.D.; Forjanic, M. Surface roughness of different dental materials before and after simulated toothbrushing in vitro. *Oper. Dent.* **2005**, *5*, 30–36.
14. Gharechahi, M.; Moosavi, H.; Forghani, M. Effect of surface roughness and materials composition. *J. Biomater. Nanobiotechnol.* **2012**, *3*, 541–546. [[CrossRef](#)]
15. Ceyhan, D.; Akdik, C.; Kirzioglu, Z. An educational programme designed for the evaluation of effectiveness of two tooth brushing techniques in preschool children. *Eur. J. Paediatr. Dent.* **2018**, *19*, 181–186.
16. Lussi, A.; Schlueter, N.; Rakhmatullina, E.; Ganss, C. Dental erosion: An overview with emphasis on chemical and histopathological aspects. *Caries Res.* **2011**, *45*, 2–12. [[CrossRef](#)]
17. Tellefsen, G.; Liljeborg, A.; Johannsen, G. How do dental materials react on tooth brushing? *Dentistry* **2005**, *5*, 341–346. [[CrossRef](#)]
18. *ISO-Standards ISO 4049*; Dentistry Polymer-Based Restorative Materials. International Organization for Standardization: Geneva, Switzerland, 2019; pp. 1–28.
19. Zamfirova, G.; Dimitrova, A. Some methodological contributions to the Vickers microhardness technique. *Polym. Test.* **2000**, *19*, 533–542. [[CrossRef](#)]
20. Mazzoleni, S.; Gargani, A.; Parciannello, R.G.; Pezzato, L.; Bertolini, R.; Zuccon, A.; Stellini, E.; Ludovichetti, F.S. Protection against dental erosion and the remineralization capacity of non-fluoride toothpaste, fluoride toothpaste and fluoride varnish. *Appl. Sci.* **2023**, *13*, 1849. [[CrossRef](#)]
21. *ISO 4288:1996*; Geometrical Product Specifications (GPS)—Surface Texture: Profile Method—Rules and Procedures for the Assessment of Surface Texture. ISO: Geneva, Switzerland, 1996.
22. Ludovichetti, F.S.; Lucchi, P.; Zambon, G.; Pezzato, L.; Bertolini, R.; Zerman, N.; Stellini, E.; Mazzoleni, S. Depth of cure, hardness, roughness and filler dimension of bulk-fill flowable, conventional flowable and high-strength universal injectable composites: An in vitro study. *Nanomaterials* **2022**, *12*, 1951. [[CrossRef](#)]
23. Sampaio, C.S.; Chiu, K.J.; Farrokhanesh, E.; Janal, M.; Puppini-Rontani, R.M.; Giannini, M.; Bonfante, E.A.; Coelho, P.G.; Hirata, R. Microcomputed tomography evaluation of polymerization shrinkage of Class I flowable resin composite restorations. *Oper. Dent.* **2017**, *42*, E16–E23. [[CrossRef](#)]
24. Vichi, A.; Margvelashvili, M.; Goracci, C.; Papacchini, F.; Ferrari, M. Bonding and sealing ability of a new self-adhering flowable composite resin in class I restorations. *Clin. Oral. Investig.* **2013**, *17*, 1497–1506. [[CrossRef](#)]
25. Garouschi, S.; Vallittu, P.; Shinya, A.; Lassila, L. Influence of increment thickness on light transmission, degree of conversion and micro hardness of bulk-fill composites. *Odontology* **2016**, *104*, 291–297. [[CrossRef](#)]
26. Ünal, M.; Candan, M.; İpek, İ.; Küçükoflaz, M.; Özer, A. Evaluation of the microhardness of different resin-based dental restorative materials treated with gastric acid: Scanning electron microscopy–energy dispersive X-ray spectroscopy analysis. *Microsc. Res. Tech.* **2021**, *84*, 2140–2148. [[CrossRef](#)]
27. Azizi, F.; Ezoji, F.; Khafri, S.; Esmaili, B. Surface micro-hardness and wear resistance of a self-adhesive flowable composite in comparison to conventional flowable composites. *Front. Dent.* **2023**, *20*, 10. [[CrossRef](#)]
28. Rashidian, A.; Saghiri, M.A.; Bigloo, S.M.; Afsharianzadeh, M. Effect of fluoride gel on microhardness of flowable composites: An in vitro study. *J. Dent. Sch. Shahid Beheshti Univ. Med. Sci.* **2014**, *32*, 16–22.
29. Czasch, P.; Ilie, N. In-vitro comparison of mechanical properties and degree of cure of a self-adhesive and four novel flowable composites. *J. Adhes. Dent.* **2013**, *42*, 131–137.
30. Cabello Malagón, I.; Cánovas Hernández, B.; Martínez Hernández, E.; Serna-Muñoz, C.; Pérez-Silva, A.; Ortiz-Ruiz, A.J. Analysis of the porosity and microhardness of glass ionomer cements. *Mater. Sci.* **2022**, *28*, 113–119. [[CrossRef](#)]
31. Yin, I.X.; Zhao, I.S.; Mei, M.L.; Li, Q.; Yu, O.Y.; Chu, C.H. Use of silver nanomaterials for caries prevention: A concise review. *Int. J. Nanomed.* **2020**, *15*, 3181–3191. [[CrossRef](#)]
32. Sidhu, S.K.; Nicholson, J.W. A review of glass-ionomer cements. *Clin. Dent. J. Funct. Biomater.* **2016**, *7*, 16.
33. Nair, V.S.; Sainudeen, S.; Padmanabhan, P.; Vijayashankar, L.V.; Sujathan, U.; Pillai, R. Three-dimensional evaluation of surface roughness of resin composites after finishing and polishing. *J. Conserv. Dent.* **2016**, *19*, 5–91.
34. Mulic, A.; Fredriksen, Ø.; Jacobsen, I.D.; Tveit, A.B.; Espelid, I.; Crossner, C.G. Dental erosion: Prevalence and severity among 16-year-old adolescents in Troms, Norway. *Eur. J. Paediatr. Dent.* **2016**, *17*, 197–201.
35. Pini, N.I.; Lima, D.A.; Lovadino, J.R.; Ganss, C.; Schlueter, N. In vitro efficacy of experimental chitosan-containing solutions as anti-erosive agents in enamel. *Caries Res.* **2016**, *50*, 337–345. [[CrossRef](#)]
36. Cruz, N.V.; Pessan, J.P.; Manarelli, M.M.; Souza, M.D.; Delbem, A.C. In vitro effect of low-fluoride toothpastes containing sodium trimetaphosphate on enamel erosion. *Arch. Oral. Biol.* **2015**, *60*, 1231–1236. [[CrossRef](#)]
37. Kelten, O.S.; Hepdeniz, O.K.; Tuncer, Y.; Kankaya, D.A.; Gurdal, O. Effect of surface characteristic of different restorative materials containing glass ionomer on *Streptococcus mutans* biofilm. *Niger. J. Clin. Pract.* **2020**, *23*, 957–964.
38. Alijamhan, A.; Habib, S.R.; AlSarhan, M.A.; AlZahrani, B.; AlOtaibi, H.; AlSunaidi, N. Effect of finishing and polishing on the surface roughness of bulk-fill composites. *Open Dent. J.* **2021**, *15*, 25–31. [[CrossRef](#)]



39. Marghalani, H.Y. Effect of filler particles on surface roughness of experimental composite series. *J. Appl. Oral. Sci.* **2010**, *18*, 59–67. [[CrossRef](#)]
40. Yap, A.U.J.; Teo, J.C.M.; Teoh, S.H. Comparative wear resistance of reinforced glass ionomer restorative materials. *Oper. Dent.* **2000**, *26*, 343–348.
41. Dionysopoulos, D.; Tolidis, K.; Sfeikos, T.; Karanasiou, C.; Parisi, X. Evaluation of surface microhardness and abrasion resistance of two dental glass ionomer cement materials after radiant heat treatment. *Adv. Mater. Sci. Eng.* **2017**, *2017*, 1–9. [[CrossRef](#)]
42. Ruivo, M.A.; Pacheco, R.R.; Sebold, M.; Giannini, M. Surface roughness and filler particles characterization of resin-based composites. *Microsc. Res. Tech.* **2019**, *82*, 1756–1767. [[CrossRef](#)]
43. Amura, Y.; Kakuta, K.; Ogura, H. Wear and mechanical properties of composite resins consisting of different filler particles. *Odontology* **2013**, *101*, 156–169.
44. O'Neill, C.; Kreplak, L.; Rueggeberg, F.A.; Labrie, D.; Shimokawa, C.A.K.; Price, R.B. Effect of tooth brushing on gloss retention and surface roughness of five bulk-fill resin composites. *J. Esthet. Restor. Dent.* **2018**, *30*, 59–69. [[CrossRef](#)]

**Disclaimer/Publisher's Note:** The statements, opinions and data contained in all publications are solely those of the individual author(s) and contributor(s) and not of MDPI and/or the editor(s). MDPI and/or the editor(s) disclaim responsibility for any injury to people or property resulting from any ideas, methods, instructions or products referred to in the content.